Structures and dissolution behaviors of $CaO-P_2O_5-TiO_2/Nb_2O_5$ ($Ca/P \geq 1$) invert glasses

Sungho Lee[1], Hirotaka Maeda[1], Akiko Obata[1], Kyosuke Ueda[2], Takayuki Narushima[2], Toshihiro Kasuga[1*]

[1] Department of Frontier Materials, Graduate School of Engineering, Nagoya Institute of Technology, Gokiso-cho, Showa-ku, Nagoya 466-8555, Japan

[2] Department of Metallurgy, Materials Science and Materials Processing, Graduate School of Engineering, Tohoku University, 6-6-02 Aoba, Aramaki, Aoba-ku, Sendai 980-8579, Japan

* Corresponding author: Tel./Fax: +81 52 735 5288

E-mail address: kasuga.toshihiro@nitech.ac.jp

Abstract

Common phosphate glasses—for example, those in the metaphosphate region—show potential as biodegradable materials. Some applications, such as biocompatible thin films coated on titanium or its alloys using radiofrequency magnetron sputtering methods, require films with good chemical durability. In the present work, CaO-P_2O_5-TiO_2/Nb_2O_5 glasses with a Ca/P ratio of ≥ 1.00 were prepared using a melt-quenching method, and their structures and dissolution behaviors were investigated. When the Ca/P ratio was increased, the amount of orthophosphate (Q_p^0) group in the glasses increased, and that of pyrophosphate (Q_p^1) group decreased. The amount of Q_p^0 group was greater than the amount of Q_p^1 groups in glasses with a Ca/P ratio of ≥ 1.14. Intermediate oxides (*i.e.*, TiO_2 and Nb_2O_5) in the glasses cross-linked with the phosphate groups to form P-O-Ti/Nb bonds; these bonds were expected to take a tetrahedral form. The glasses prepared in the present work showed excellent chemical durability, because of the P-O-Ti/Nb bonds and the delocalized P=O bonds that resulted from the increasing Q_p^0 content in the glasses.

Highlights

- Phosphate glasses including numerous orthophosphate groups (Q_p^0) were prepared
- The number of P-O-Ti/Nb bonds increased with increasing Q_p^0 content in the glasses
- TiO_x/NbO_y groups formed tetrahedrons in the glasses including numerous Q_p^0 groups
- The chemical durability increased with increasing Q_p^0 content in the glasses

Keywords

Biomaterial, calcium phosphate glass, invert glass, structure, dissolution

1. Introduction

Titanium-containing calcium phosphate invert glasses (Ti-IGs) have been a focus of research in our group [1]. Ti-IGs consist of short phosphate groups, such as ortho- and pyrophosphates (Q_p^0 and Q_p^1), because P-O-Ti bonds help to form their glass network [1]. Ti-IGs indicate *in vitro* and *in vivo* bioactivity [2,3]. Ti-IGs can be applied as a coating material for titanium or its alloys. In our previous work, Ti-IG powders were dip coated on a Ti-29Nb-13Ta-4.6Zr alloy, and then heat treated at 800°C for 1 h. The resulting layer were 10 ~ 20 μm in thickness, without significant cracks, and the tensile bonding strength between the layer and the substrate was measured to be 26 MPa [4]. Recently, niobium-containing calcium phosphate invert glasses (Nb-IGs) were prepared by our group [5,6]. Crystallized Nb-IGs showed apatite-forming abilities in simulated body fluids [5]. Trace amounts of Nb^{5+} ions (0.04 ~ 0.06 mM) dissolved from the Nb-IGs enhanced the differentiation of osteoblast-like cells, such as alkali phosphatase (ALP) activity [6]. Tamai *et al.* reported that Nb^{5+} ions enhanced calcification, because of the enhancement of the ALP activity [7].

Narushima *et al.* reported an amorphous calcium phosphate film prepared on metallic titanium using a radiofrequency magnetron sputtering (RF-sputtering) method [8]. The tensile strength of the bond between the film and the titanium was greater than

60 MPa when the coating layer thickness was between 0.5 and 1 μm (the epoxy glue used in the test was detached without damage to the film) [9]. The bonding strength decreased to 30 MPa after the amorphous calcium phosphate film on the titanium was immersed in phosphate-buffered saline (PBS) for 3 days, because of the low chemical durability of the film [10]. Amorphous films on metallic titanium or its alloys are required to have excellent chemical durability and excellent biocompatibility.

Ti-IGs and Nb-IGs may be candidate for the amorphous film using RF-sputtering method. To fully realize the application of method for Ti-IGs and Nb-IGs, it is necessary to clarify their (Ti-IGs and Nb-IGs) dissolution behaviors. In this work, we focused on phosphate invert glasses containing TiO_2 or Nb_2O_5 and large amounts of CaO (where the invert glasses were prepared via conventional melt-quenching), and examined their structures and dissolution behaviors.

2. Materials and methods

2.1 Preparation of the glasses

Titanium- or niobium-containing calcium phosphate invert glasses with nominal compositions of xCaO·(90-x)P_2O_5·10TiO_2 (mol%, x = 60 to 66, denoted here as Ti-IGs)

and yCaO·(94.5-y)P_2O_5·5.5Nb_2O_5 (mol%, y = 63 to 68.5, denoted here as Nb-IGs) were prepared, as shown in Table 1. Glass batches were prepared using $CaCO_3$ (99.5%), H_3PO_4 (85% liquid), TiO_2 (99.5%), and Nb_2O_5 (99.9%). All reagents were obtained from Kishida Chemical Co., Japan. The glass compositions were adjusted by changing the atomic ratios of Ca, P, and Ti or Nb. The reagents were mixed with distilled water to make a slurry at room temperature. After the mixture was dried under an infrared lamp overnight and then stored at 140°C, it was melted in a platinum crucible at 1500°C for 30 min, and then quenched via p\ressing, which was applied using two stainless-steel plates, to prevent crystallization. The resulting glass compositions were examined using inductively coupled plasma atomic emission spectroscopy (ICP-AES, ICPS-7000, Shimadzu Co., Japan) for the Ti-IGs, using aqueous solutions in which 5 mg of the glass powders was dissolved in 20 mL of 1N HCl (n = 3). The compositions of the Nb-IGs were analyzed using energy dispersive X-ray spectroscopy (EDX, JCM-6000 and JED-2300, JEOL Co., Japan): the glass fractures were coated with amorphous osmium using plasma chemical vapor deposition equipment (n = 3).

2.2 Thermal analysis

The glass transition temperature (T_g) and crystallization temperature (T_c, defined

as the onset of crystallization) of the glasses were obtained using differential thermal analysis (DTA; heating rate: 5 K/min, Thermo plus TG8120, Rigaku Co., Japan). The glassification degree—which is defined as $(T_c - T_g)/T_g$ (K/K) [11], and is used as an indicator of the glass-forming ability—was calculated.

2.3 Characterization of the glass structure

The glass structure was investigated using laser Raman spectroscopy, which was performed on quenched glass samples in the Raman shift region between 500 and 1300 cm^{-1} (NRS-3300, JASCO Co., Japan). The samples were excited by the 532.08 nm line of Nd:YAG solid-state laser with 6.4 mW of power at room temperature. The exposure time was 10 sec and the cumulated number was 8. The resolution of Raman spectra is 4.13 cm^{-1}.

The glass samples were pulverized to the powder for solid-state ^{31}P magic angle spinning nuclear magnetic resonance (MAS-NMR) spectra. ^{31}P MAS-NMR spectra were measured to determine the phosphate structures in the glasses at 161.906 MHz in a 8 mm rotor that was spinning at 5 kHz (Varian UNITY Inova 400 plus). A single pulse experiment with 5 μs pulse width, 60 s recycle delay, and a cumulative number of 64, was performed for each sample. The chemical shift was referenced to the signal of $NH_4H_2PO_4$

as 1.0 ppm. The theoretical network connectivity (NC_{theor}), which is defined as the number of bridging oxygens per network forming element [12], was calculated using the following equation,

$$NC_{theor} = \frac{3[P_2O_5]-[CaO]-(2[TiO_2]\ or\ 3[Nb_2O_5])}{[P_2O_5]} \quad , \quad (1)$$

where $[P_2O_5]$, $[CaO]$, $[TiO_2]$, and $[Nb_2O_5]$ are the molar fractions of phosphate, calcium oxide, titanium dioxide, and niobium pentoxide, respectively. The experimental network connectivity (NC_{exp}) was calculated based on the deconvolution of ^{31}P MAS-NMR spectra, assuming the presence of Q_p^0 and Q_p^1 units.

The glasses density were measured by the Archimedes' method using water as immersion fluid at room temperature: the glass fractures were prepared 100 ~ 300 mg and the water temperature was 25°C (n = 3). The oxygen density was calculated, to allow the calculation of the compactness of the glass network using the following equation [13,14]:

$$\rho_{oxygen} = \frac{M(O)\times\{[CaO]+5[P_2O_5]+(2[TiO_2]\ or\ 5[Nb_2O_5])\}}{M(glass)/\rho_{glass}}, \quad (2)$$

where *M(O)* and *M(glass)* are the atomic weight of oxygen and the molar weight of the glass, respectively; $[CaO]$, $[P_2O_5]$, $[TiO_2]$, and $[Nb_2O_5]$ are the molar fractions of phosphate, calcium oxide, titanium dioxide, and niobium pentoxide, respectively; and ρ_{glass} is the experimental density of the glass.

2.4 Characterization of dissolution in a Tris buffer solution

Glass samples were pulverized and sieved to provide particle sizes between 125 and 300 μm. A Tris buffer solution was prepared by dissolving 6.118 g of tris(hydroxymethyl)aminomethane ($NH_2C(CH_2OH)_3$, Kishida Chemical Co., Japan) in 1 L of distilled water at 37°C, and adjusting the pH to 7.4. Fifteen milligrams of the glass powders was soaked in 15 mL of the Tris buffer solution at 37°C for 7 days (n = 3). The concentrations of Ca^{2+}, P^{5+}, Ti^{4+}, and Nb^{5+} ions in the solution were measured using ICP-AES.

3. Results

3.1 Glass formation

Optically clear glasses were obtained in the composition region with a Ca/P ratio of < 1.10 (nominal composition), while partially crystallized glasses were obtained with Ca/P ratios of ≥ 1.10. In the subsequent experiments, crystalline (opaque) parts were removed manually. ICP-AES analysis showed that the composition of the Ti-IGs was very close to the nominal composition, as shown in Table 1. The Nb-IGs, however, could not

be analyzed using ICP-AES, because the glass powders turned into a gel in acids such as 1N HCl and 1N HNO_3. The compositions of the Nb-IGs were therefore analyzed using EDX (Table 1); the amount of phosphorus was reasonably close to that shown in the nominal composition, and the amounts of calcium and niobium varied by approximately 2.5 mol%. Because the phosphorus $K\alpha$ (2.013 eV) and niobium $L\alpha$ (2.166 eV) peaks overlapped, it was difficult to accurately determine the composition. Hereafter, the glass codes (Ca/P ratio) estimated from the nominal compositions, are used in the discussion of the results.

3.2 Thermal properties

Figure 1 shows results for T_g, T_c, and the glassification degree for the glasses. T_g and T_c showed increasing trends with increases in the Ca/P ratio; the T_g values varied in the region of 646°C to 684°C and 645°C to 684°C for the Ti-IGs and Nb-IGs, respectively, and the T_c values varied in the region of 714°C to 735°C and 722°C to 737°C for the Ti-IGs and Nb-IGs, respectively. The glassification degree showed decreasing trends with increases in the Ca/P ratio; the values for the Ti-IGs varied between 0.05 and 0.08, and the values for the Nb-IGs varied between 0.06 and 0.09.

3.3 Glass structures

The phosphate groups in the glasses showed Raman bands corresponding to Q_p^0 and Q_p^1 groups, as shown in Fig. 2 (a, b), including the POP_{sym} stretching mode of the bridging oxygen in Q_p^1 (750 cm^{-1}), the $(PO_4)_{sym}$ stretching mode of the non-bridging oxygen in Q_p^0 (950 cm^{-1}), the $(PO_3)_{sym}$ stretching vibrations of the non-bridging oxygen in Q_p^1 (1040 cm^{-1}) [15], and the P-O stretching of the Q_p^1 chain terminator (1115 cm^{-1}) [16]. The Ti-IGs showed bands corresponding to the Ti-O stretching vibrations of TiO_6 octahedrons (640 cm^{-1}), the Ti-O stretching vibrations of TiO_4 tetrahedrons (875 cm^{-1}) [17], and P-O-Ti bonds (993 cm^{-1}) [1,18,19]. The Nb-IGs showed bands corresponding to the Nb-O vibrations of NbO_6 octahedrons corner-linked in a three-dimensional network (640 cm^{-1}) [20,21], the Nb-O vibrations of NbO_4 tetrahedrons (845 cm^{-1}) [21], the Nb-O bond vibrations in isolated NbO_6 octahedral units (910 cm^{-1}) [20,21], and the Nb=O stretching vibration mode of the NbO_4 terminal bond (990 cm^{-1}) [22]. The experimental Raman bands were simulated, assuming Gaussian lines. The integrated peak intensities of the deconvoluted bands were calculated; the integrated peak intensities of the phosphate, Ti-O, and Nb-O group bands were normalized by the sums $I(POP_{sym})$ + $I((PO_4)_{sym})$ + I(P-O-Ti) + $I((PO_3)_{sym})$ + I(P-O stretch Q_p^1 chain terminator), and $I(TiO_6)$ + $I(TiO_4)$ + I(P-O-Ti) and $I(NbO_{6\_3D})$ + $I(NbO_4)$ + $I(NbO_{6\_isolated})$ + I(Nb=O bond of

$NbO_{4\_terminal}$), respectively (Fig. 2 (c-f)), where *I* denotes each peak amplitude. With increases in the Ca/P ratio in the Ti-IGs, the integrated peak intensities associated with the Q_p^0 group and the P-O-Ti bonds increased, and those associated with the Q_p^1 group decreased (Fig. 2 (c)). With increases in the Ca/P ratio in the Nb-IGs, the integrated peak intensities associated with the Q_p^0 group increased, and those associated with the Q_p^1 group decreased (Fig. 2 (d)). With increases in the Ca/P ratio in the Ti-IGs, the peak intensity associated with the TiO_4 tetrahedrons showed no significant changes, the peak intensity associated with the P-O-Ti bonds increased, and the peak intensity associated with the TiO_6 octahedrons decreased (Fig. 2 (e)); with increases in the Ca/P ratio in the Nb-IGs, the peak intensity associated with the NbO_4 tetrahedrons increased, and the peak intensity associated with the NbO_6 octahedrons decreased (Fig. 2 (f)).

^{31}P MAS-NMR spectra of the glasses are shown in Fig. 3 (a, b). The center peaks between 10 and −25 ppm were assigned to Q_p^0 and Q_p^1 units, and the remaining peaks observed on both sides of the center peaks were associated with spinning side bands. The experimental spectra were simulated, assuming Gaussian lines for the Q_p^0 and Q_p^1 units. With increases in the Ca/P ratio, the fractured peak top positions of Q_p^0 low-field shifted from 0.8 to 2.0 ppm and from 0.6 to 2.2 ppm for the Ti-IGs and the Nb-IGs, respectively, and the fractured peak top positions of Q_p^1 low-shifted from −6.9 to −2.7 ppm and from

−7.0 to −2.1 ppm for the Ti-IGs and the Nb-IGs, respectively, as shown in Fig. 3 (c, d). The peak integrated portions associated with the Q_p^0 and Q_p^1 groups in the glasses increased and decreased linearly, respectively, with increases in the Ca/P ratio. With increases in the Ca/P ratio, the Q_p^0 contents in the Ti-IGs and Nb-IGs increased from 33% to 66% and from 33% to 67%, respectively, and the Q_p^1 contents in the Ti-IGs and Nb-IGs decreased from 67% to 34% and from 67% to 33%, respectively, as shown in Fig. 3 (e, f).

Figure 4 shows the experimental and theoretical network connectivities of the glasses. With increases in the Ca/P ratio, NC_{theor} for the Ti-IGs and the Nb-IGs decreased from 0.33 to -0.23 and from 0.51 to -0.21, respectively, and NC_{exp} for the Ti-IGs and the Nb-IGs decreased from 0.67 to 0.34 and from 0.67 to 0.33, respectively.

3.4 Density of the glasses

The density of the Ti-IGs and the Nb-IGs increased from 3.00 to 3.05 $g \cdot cm^{-3}$ and from 3.08 to 3.15 $g \cdot cm^{-3}$, respectively, with increases in the Ca/P ratio, as shown in Fig. 5 (a). No significant difference in the oxygen density of the glasses was observed, only a slight decrease; the oxygen density in the Ti-IGs varied between 1.29 and 1.32 $g \cdot cm^{-3}$, and that in the Nb-IGs varied between 1.18 and 1.21 $g \cdot cm^{-3}$.

3.5 Dissolution behaviors of the glasses

Figure 6 shows ion-release percentages from the glasses into the Tris buffer solution, relative to the original amount in the glasses. The solubility of the glasses was very low; less than 5% and 7% of all of the components were released from the Ti-IGs and the Nb-IGs, respectively, even after 7 days. With increases in the Ca/P ratio, the ion-release percentage for the Ti-IGs and Nb-IGs decreased from 5.0% to 3.5% and from 7.0% to 5.0%, respectively.

4. Discussion

4.1 Glassification degree

T_g and T_c increased for the Ti-IGs and the Nb-IGs—and their glassification degree decreased—with increases in the Ca/P ratio. The glasses showed low glassification degrees; a value of 0.05 was determined for the Ti-IGs (Ca/P = 1.24), and a value of 0.06 was determined for the Nb-IGs (Ca/P = 1.30). The glassification degree is an indication of the glass-forming ability; Ouchetto *et al.* reported a glassification degree of approximately 0.25 for a zinc metaphosphate glass, and a low value of approximately

0.07 for an invert glass [11]. The results obtained here showed that the Ti-IGs and Nb-IGs had a tendency to induce crystallization during quenching, owing to insufficient amounts of a glass network former (*i.e.,* phosphate).

With increases in the Ca/P ratio, the integrated peak intensity associated with the Q_p^0 group increased, and that associated with the Q_p^1 group decreased. The peak integrated portions for the phosphate groups (determined from the ^{31}P MAS-NMR spectra for the Ti-IGs and Nb-IGs) showed that the Q_p^0 content increased to 66% and 67%, and the Q_p^1 content decreased to 34% and 33%, respectively, with increases in the Ca/P ratio. The laser Raman and ^{31}P MAS-NMR spectra indicated a similar tendency; that is, increases in the Q_p^0 group content and decreases in the Q_p^1 group content. The Ca/P ratio of the glasses with $Q_p^0/Q_p^1 = 1$ in the integrated peak portion for Ti-IGs or Nb-IGs was 1.10 or 1.14, respectively. As shown in Fig. 1, the glasses containing larger amounts of Q_p^0 group than Q_p^1 group (*i.e.*, Ti-IGs with Ca/P ≥ 1.10, and Nb-IGs with Ca/P ≥ 1.14) showed a glassification degree of 0.05 ~ 0.07; nearly clear glasses with partially crystallized portions were obtained.

4.2 Glass structure

The glass density increased with increases in the Ca/P ratio, despite the decrease

in *M(glass)*, and the oxygen density of the glasses showed very little change (or decreased slightly). These results indicated that the glass networks became more densely packed with increases in the Ca/P ratio. Intermediate oxides—*i.e.*, TiO_2, and Nb_2O_5—would have assisted in the formation of the glass network structure, even in the glasses containing numerous Q_p^0 group, although predictably their glass network would change to be less densely packed.

The NC_{theor} values calculated using equation (1) were less than 0 with Ca/P ratios of > 1.13 and > 1.21 for the Ti-IGs and Nb-IGs, respectively; this meant that, theoretically, no glass network structure could form in these composition regions. That is, the intermediate oxides helped to form the glass network structure. The NC_{exp} values were 0.34 and 0.33 for the Ti-IGs and Nb-IGs, respectively. Polyhedral TiO_n or NbO_n would have cross-linked the phosphate groups. Our previous work showed that Ti-IGs contain P-O-Ti bonds, and that the peak intensity in the Raman spectra increased with increases in the TiO_2 content [1]. Brow *et al.* and Segawa *et al.* reported P-O-Ti bonds in binary TiO_2-P_2O_5 glasses [18] and TiO_2-ZnO-P_2O_5 glasses [19]. Jazouli *et al.* and Mazali *et al.* reported P-O-Nb bonds in Na_2O-P_2O_5 glasses modified with a small amount of Nb_2O_5 [23], and in niobophosphate glasses containing predominantly Q_p^0 and Qp^1 groups [24]. In the present glass system, the integrated peak intensity associated with the P-O-Ti bonds

increased with increases in the Ca/P ratio in the Ti-IGs; it is possible that the formation of P-O-Nb bonds increased with increases in the Ca/P ratio in the Nb-IGs.

T_g values of the glasses were increased with increasing the Ca/P ratio, *i.e.*, NC_{theor} and NC_{exp} were decreased. A similar trend has been observed for the glasses in the P_2O_5-MgO [25] and the P_2O_5-CaO-Na_2O [26] system. Mandlule *et al.* reported, this trend can be explained by an increasing ionic contribution in the glass structure [26]. Glasses with low phosphate content, *i.e.*, invert glasses, formed their network by interactions between short phosphate units and modifier ions [26]. Brow reported, invert glasses do not have a continuous random network and their structure consist of short phosphate unit and modifier ions linked through non-bridging oxygens [27]. The structures of the invert glasses were more influenced by $P\text{-}O^-\ Me^+$ (Me^+ being a modifier oxide) inter-chain cross-links than P-O-P bond [26,27]. Q_p^0 group in the glasses were increased with increasing the Ca/P ratio, *i.e.*, number of non-bridging oxygen in the glasses were increased. The increasing number of non-bridging oxygen in the glasses caused the increase in their T_g, due to increase ionic contribution.

As shown in Fig. 3, the fractured peak top position associated with the phosphate groups showed a low-field shift with increases in the Ca/P ratio, which indicated a decrease in the electron density. Electrons belonging to the Q_p^0 and Q_p^1 groups were

pulled to the titanium or niobium side; the electron densities of the Q_p^0 and Q_p^1 groups therefore decreased with increases in the Ca/P ratio. Because the amount of P-O-Ti or P-O-Nb bonds in the glasses increased, the Q_p^0 and Q_p^1 groups had more chance to be influenced by the titanium or niobium, which have larger field strengths compared with calcium (Nb : 1.73, Ti : 1.04, Ca : 0.33 valence/Å^2) [28].

The integrated intensities associated with TiO_4 showed no significant difference when the Ca/P ratio in the Ti-IGs was increased; in contrast, the intensity associated with P-O-Ti increased, and that associated with TiO_6 decreased. The linking of the TiO_4 to the phosphate groups might have increased as a result of the decreases in the intensity associated with TiO_6. Brow *et al.* and Segawa *et al.* reported that titania linking to phosphate groups takes TiO_6 octahedron structure [18,19] in the CaO-TiO_2-P_2O_5 and TiO_2-ZnO-P_2O_5 glasses, respectively, consisting of Q_p^2 and Q_p^1 groups. Li *et al.* reported that, in P_2O_5-CaO-Na_2O-TiO_2 pyrophosphate glasses, titania enters the glass network as TiO_4 tetrahedrons connected to phosphate groups through P-O-Ti bonds [29]. Nagarjuna *et al.* reported that Ti^{4+} ions enter the glass network as TiO_4 units and form the linkage of P-O-Ti bonds [30]. In the Nb-IGs, the integrated intensity associated with NbO_6 decreased with increases in the Ca/P ratio, and that associated with NbO_4 increased. Niobate linking to P-O-Nb bond takes NbO_6 octahedron structure, when the glasses were composed of

Q_p^2 and Q_p^1 groups [23,24,31]. Chu *et al.* and Hsu *et al.* reported that P-O-Nb bonds formed, and the partial NbO_6 octahedron structure gradually turned into a NbO_4 tetrahedron structure, with decreases in the content of P_2O_5 in the glasses [21,32]. The present glasses consisted of Q_p^0 and Q_p^1 groups; with Ca/P ratios ≥ 1.10 in the Ti-IGs and ≥ 1.14 in the Nb-IGs, they consisted predominantly of Q_p^0 groups. In the glasses with a Ca/P ratio of ~1.00, which consisted predominantly of Q_p^1 groups, TiO_6 or NbO_6 octahedrons cross-linked the phosphate groups to form P-O-Ti/Nb bonds. In Q_p^0-predominant compositions, *i.e.*, in Ti-IGs with Ca/P ≥ 1.10 and Nb-IGs with Ca/P ≥ 1.14, the intermediate oxides took the form of tetrahedrons and cross-linked the phosphate groups.

4.3 Dissolution behaviors of the glasses

The glasses showed good chemical durability (up to 5% or 7% dissolution from the Ti-IGs or Nb-IGs after 1 week, respectively). Brauer *et al.* and Kishioka *et al.* reported that the chemical durability of P_2O_5-CaO-MgO-Na_2O-TiO_2 and Na_2O/K_2O-TiO_2-P_2O_5 glasses was improved by increases in the TiO_2 content, because the formed P-O-Ti bonds impeded the hydration of the phosphate groups [12,33]. Mazali *et al.* reported that the chemical durability of Li_2O-Nb_2O_5-CaO-P_2O_5 glasses was improved by the formation of

P-O-Nb bonds [24]. Masai *et al.* reported that the chemical durability of SrO-BaO-Nb_2O_5-P_2O_5 glasses was improved by increasing the Q_p^0 content in the glasses, as a result of delocalization of the P=O groups [34]. The chemical durability of the glasses was improved when the Ca/P ratio was increased, because the number of P-O-Ti/Nb bonds and delocalized P=O bonds increased with increases in the Q_p^0 content in the glasses. All of the components in the glasses dissolved at similar rates; the glasses showed congruent dissolution, which indicated that no selective ion leaching occurred. It is expected that it will be facile to control the ion dissolution behavior of the present glasses, because of their excellent chemical durability.

5. Conclusion

The structures and dissolution behaviors of glasses containing TiO_2 or Nb_2O_5 and large amounts of CaO were investigated. Glasses with a Ca/P ratio of ≥ 1.00 were successfully prepared using a conventional melt-quenching method. In the glasses with compositions of Ca/P > 1.10 in the Ti-IGs and Ca/P > 1.14 in the Nb-IGs, the amount of Q_p^0 group was larger than the amount of Q_p^1 group. In the glasses with high Q_p^0 contents, the intermediate oxides (TiO_2, Nb_2O_5) took the form of tetrahedrons (a shape similar to

that of the Q_p^0 group), and cross-linked the phosphate groups. The chemical durability of the glasses increased with increases in the Ca/P ratio, because the number of P-O-Ti/Nb bonds and Q_p^0 groups, which delocalized the P=O bonds, increased. The present glass system shows potential as a candidate for the preparation of thin films on metal surfaces via RF-sputtering, because of its excellent chemical durability.

Acknowledgments

This work was supported in part by Japan Society for the Promotion of Science KAKENHI Grant Numbers 25249094, 26289238, and 267992.

References

[1] T. Kasuga, Y. Abe, Calcium phosphate invert glasses with soda and titania, J. Non-Cryst. Solids 243 (1999) 70–74.

[2] T. Kasuga, Y. Hosoi, M. Nogami, M. Niinomi, Apatite formation on calcium phosphate invert glasses in simulated body fluid, J. Am. Ceram. Soc. 84 (2001) 450–452.

[3] T. Kasuga, T. Hattori, M. Niinomi, Phosphate glasses and glass-ceramics for biomedical applications, Phosphorus Res. Bull., 26 (2012) 8–15.

[4] T. Kasuga, M. Nogami, M. Niinomi, Joining of calcium phosphate invert glass-ceramics on a β-type titanium alloy, J. Am. Ceram. Soc. 86 (2003) 1031–1033.

[5] H. Maeda, T. Miyajima, S. Lee, A. Obata, K. Ueda, T. Narushima, T. Kasuga, Preparation of calcium pyrophosphate glass-ceramics containing Nb_2O_5, J. Ceram. Soc. Jpn. 122 (2014) 122–124.

[6] A. Obata, Y. Takahashi, T. Miyajima, K. Ueda, T. Narushima, T. Kasuga, Effects of niobium ions released from calcium phosphate invert glasses containing Nb_2O_5 on osteoblast-like cell functions, ACS Appl. Mater. Interfaces 4 (2012) 5684–5690.

[7] M. Tamai, K. Isama, R. Nakaoka, T. Tsuchiya, Synthesis of a novel β-tricalcium phosphate/hydroxyapatite biphasic calcium phosphate containing niobium ions and evaluation of its osteogenic properties, J. Artif. Organs 10 (2007) 22–28.

[8] T. Narushima, K. Ueda, T. Goto, H. Masumoto, T. Katsube, H. Kawamura, C. Ouchi, Y. Iguchi, Preparation of calcium phosphate films by radiofrequency magnetron sputtering, Mater. Trans. 46 (2005) 2246–2252.

[9] U. Kyosuke, T. Narushima, T. Goto, T. Katsube, H. Nakagawa, H. Kawamura, M. Taira, Evaluation of calcium phosphate coating films on titanium fabricated using RF magnetron sputtering, Mater. Trans. 48 (2007) 307–312.

[10] U. Kyosuke, N. Takayuki, G. Takashi, T. Masayuki, K. Tomoyuki, Fabrication of calcium phosphate films for coating on titanium substrates heated up to 773 K by RF magnetron sputtering and their evaluations, Biomed. Mater. 2 (2007) S160–S166.

[11] M.Ouchetto, B. Elouadi, S. Parke, Study of lanthanide zinc phosphate glasses by differential thermal analysis, Phys. Chem. Glasses 32 (1991) 22–28.

[12] D.S. Brauer, N. Karpukhina, R.V. Law, R.G. Hill, Effect of TiO_2 addition on structure, solubility and crystallisation of phosphate invert glasses for biomedical applications, J. Non-Cryst. Solids 356 (2010) 2626–2633.

[13] N.H. Ray, Composition-property relationships in inorganic oxide glasses, J. Non-Cryst. Solids 15 (1974) 423–434.

[14] M. Tylkowski, D.S. Brauer, Mixed alkali effects in Bioglass® 45S5, J. Non-Cryst. Solids 376 (2013) 175–181.

[15] M.A. Karakassides, A. Saranti, I. Koutselas, Preparation and structural study of binary phosphate glasses with high calcium and/or magnesium content, J. Non-Cryst. Solids 347 (2004) 69–79.

[16] R.K. Brow, D.R. Tallant, S.T. Myers, C.C. Phifer, The short-range structure of zinc polyphosphate glass, J. Non-Cryst. Solids 191 (1995) 45–55.

[17] S. Sakka, F. Miyaji, K. Fukumi, Structure of binary $K_2O{\cdot}TiO_2$ and $Cs_2O{\cdot}TiO_2$ glasses, J. Non-Cryst. Solids 112 (1989) 64–68.

[18] R.K. Brow, D.R. Tallant, W.L. Warren, A. McIntyre, D.E. Day, Spectroscopic studies of the structure of titanophosphate and calcium titanophosphate glasses, Phys. Chem. Glasses 38 (1997) 300–306.

[19] H. Segawa, N. Akagi, T. Yano, S. Shibata, Properties and structures of TiO_2-ZnO-P_2O_5 glasses, J. Ceram. Soc. Jpn. 118 (2010) 278–282.

[20] A. Flambard, J.J. Videau, L. Delevoye, T. Cardinal, C. Labrugère, C.A. Rivero, M. Couzi, L. Montagne, Structure and nonlinear optical properties of sodium-niobium phosphate glasses, J. Non-Cryst. Solids 354 (2008) 3540–3547.

[21] S.M. Hsu, J.J. Wu, S.W. Yung, T.S. Chin, T. Zhang, Y.M. Lee, C.M. Chu, J.Y. Ding, Evaluation of chemical durability, thermal properties and structure characteristics of Nb-Sr-phosphate glasses by Raman and NMR spectroscopy, J. Non-Cryst. Solids 358 (2012) 14–19.

[22] J.M. Jehng, I.E. Wachs, Structural chemistry and Raman spectra of niobium oxides, Chem. Mater. 3 (1991) 100–107.

[23] A. El Jazouli, J.C. Viala, C. Parent, G. Le Flem, P. Hagenmuller, Structural investigation of glasses belonging to the Na_2O-Nb_2O_5-P_2O_5 system, J. Solid State Chem. 73 (1988) 433–439.

[24] I. Mazali, L. Barbosa, O. Alves, Preparation and characterization of new niobophosphate glasses in the Li_2O-Nb_2O_5-CaO-P_2O_5 system, J. Mater. Sci. 39 (2004) 1987–1995.

[25] G. Walter, J. Vogel, U. Hoppe, P. Hartmann, Structural study of magnesium polyphosphate glasses, J. Non-Cryst. Solids 320 (2003) 210–222.

[26] A. Mandlule, F. Döhler, L. van Wüllen, T. Kasuga, D.S. Brauer, Changes in structure and thermal properties with phosphate content of ternary calcium sodium phosphate glasses, J. Non-Cryst. Solids 392–393 (2014) 31–38.

[27] R.K. Brow, Review: the structure of simple phosphate glasses, J. Non-Cryst. Solids 263–264 (2000) 1–28.

[28] A. Dietzel, Die Kationenfeldstärken und ihre Beziehungen zu Entglasungsvorgängen, zur Verbindungsbildung und zu den Schmelzpunkten von Silicaten, Ztschr. Elektrochem. 48 (1942) 9–23.

[29] Y. Li, W. Weng, J.D. Santos, A.M. Lopes, Structural studies of Na_2O-TiO_2-CaO-P_2O_5 system glasses investigated by FTIR and FT-Raman, Phys. Chem. Glasses - Eur. J. Glass Sci. Technol. Part B 49 (2008) 41–45.

[30] M. Nagarjuna, T. Satyanarayana, Y. Gandhi, N. Veeraiah, Influence of Ag_2O on some physical properties of LiF-TiO_2-P_2O_5 glass system, J. Alloys Compd. 479 (2009) 549–556.

[31] F.F. Sene, J.R. Martinelli, L. Gomes, Synthesis and characterization of niobium phosphate glasses containing barium and potassium, J. Non-Cryst. Solids 348 (2004) 30–37.

[32] C.M. Chu, J.J. Wu, S.W. Yung, T.S. Chin, T. Zhang, F.B. Wu, Optical and structural properties of Sr-Nb-phosphate glasses, J. Non-Cryst. Solids 357 (2011) 939–945.

[33] A. Kishioka, M. Haba, M. Amagasa, Glass formation in multicomponent phosphate systems containing TiO_2, Bull. Chem. Soc. Japan 47 (1974) 2493–2496.

[34] H. Masai, R. Shirai, K. Yoshida, Y. Takahashi, R. Ihara, T. Fujiwara, Y. Tokuda, T. Yoko, ^{31}P NMR and IR Study of highly water-stable SrO-BaO-Nb_2O_5-P_2O_5 glass and glass-ceramics, Chem. Lett. 42 (2013) 1305–1307.

Figure and table captions

Figure 1: Glass transition temperature (T_g), crystallization temperature (T_c), and glassification degree (($T_c - T_g$)/T_g) for (a) Ti-IGs, and (b) Nb-IGs.

Figure 2: Laser Raman spectra for (a) Ti-IGs, and (b) Nb-IGs, and normalized integrated peak intensities corresponding to phosphate groups of (c) Ti-IGs, and (d) Nb-IGs, (e) Ti-O groups of Ti-IGs, and (f) Nb-O groups of Nb-IGs, as a function of the Ca/P ratio in the glass.

Figure 3: ^{31}P MAS-NMR spectra for (a) Ti-IGs, and (b) Nb-IGs, fractured peak top positions for (c) Ti-IGs, and (d) Nb-IGs, and peak integrated portions of phosphate groups for (e) Ti-IGs, and (f) Nb-IGs, as a function of the Ca/P ratio in the glass.

Figure 4: Experimental and theoretical network connectivities of (a) Ti-IGs, and (b) Nb-IGs, as a function of the Ca/P ratio in the glass.

Figure 5: (a) Densities of Ti-IGs and Nb-IGs, and (b) calculated oxygen densities of Ti-IGs and Nb-IGs, as a function of the Ca/P ratio in the glass.

Figure 6: Percentage of ions released into the Tris buffer solution, relative to the total amount in (a–c) Ti-IGs, and (d–f) Nb-IGs, for (a, d) Ca^{2+}, (b, e) P^{5+}, (c) Ti^{4+}, and (f) Nb^{5+} ions, as a function of the Ca/P ratio in the glass.

Table 1: Nominal and analyzed glass compositions, and nominal Ca/P ratios of the glasses (glass code). The analyzed compositions are shown in round brackets with standard deviation.

Figures

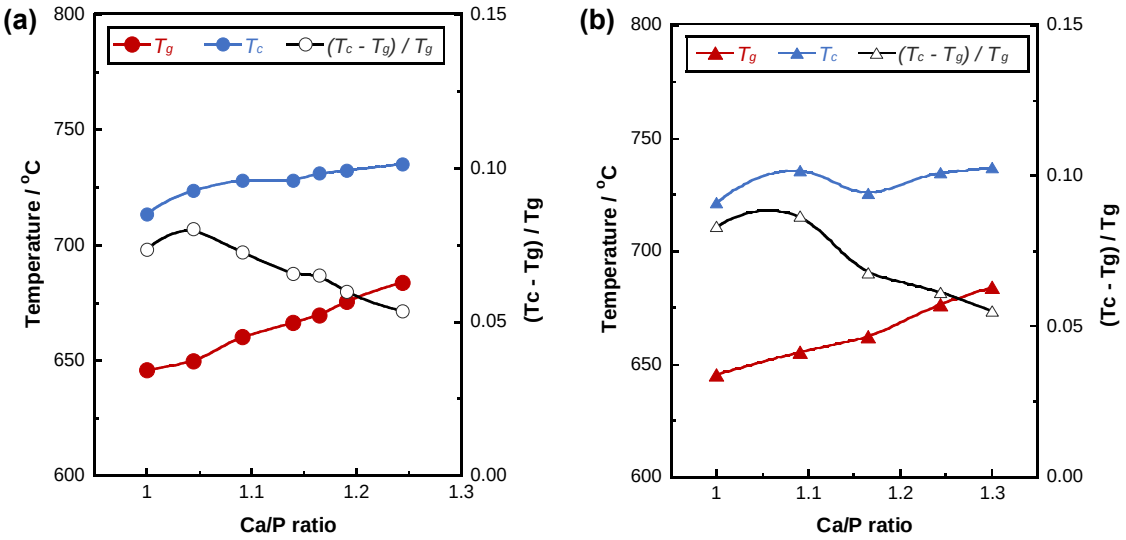

Fig. 1

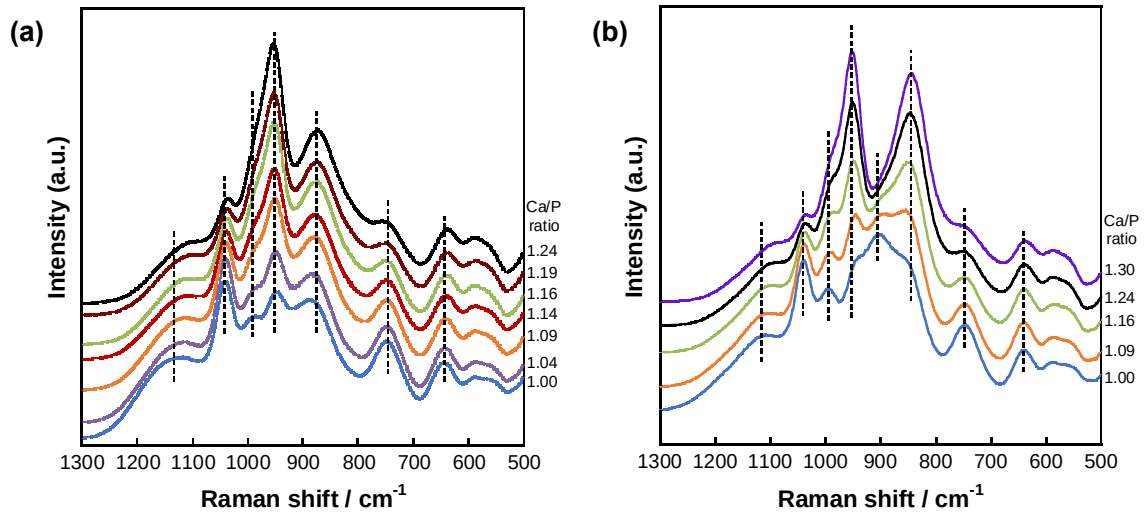
(a)
Intensity (a.u.)
Ca/P ratio
1.24
1.19
1.16
1.14
1.09
1.04
1.00
1300 1200 1100 1000 900 800 700 600 500
Raman shift / cm-1
(b)
Intensity (a.u.)
Ca/P ratio
1.30
1.24
1.16
1.09
1.00
1300 1200 1100 1000 900 800 700 600 500
Raman shift / cm-1

1

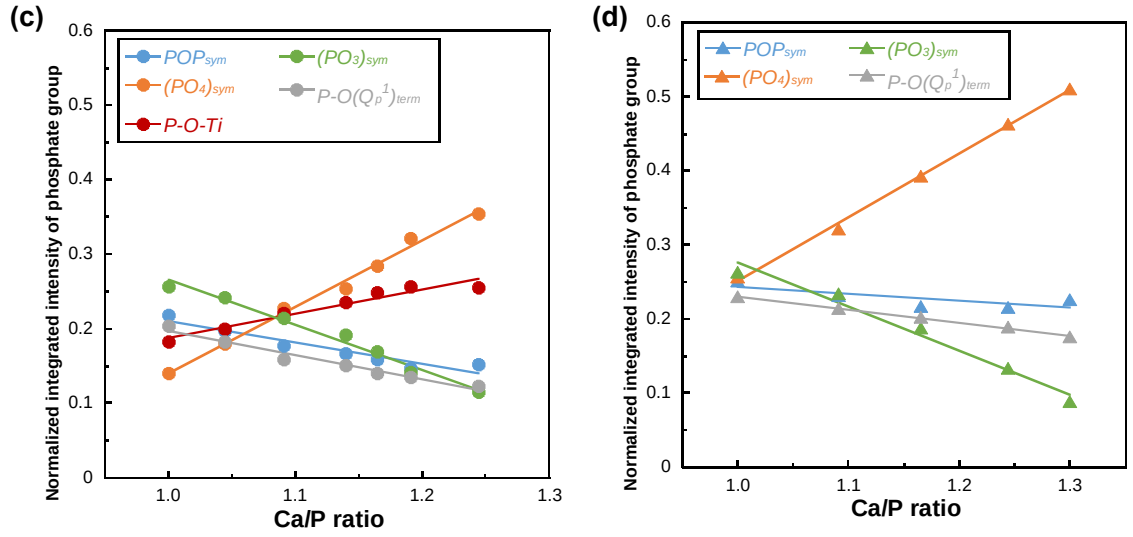
(c)
POPsym
(PO3)sym
(PO4)sym
P-O(Qp1)term
P-O-Ti
Normalized integrated intensity of phosphate group
Ca/P ratio
(d)
POPsym
(PO3)sym
(PO4)sym
P-O(Qp1)term
Normalized integrated intensity of phosphate group
Ca/P ratio

2

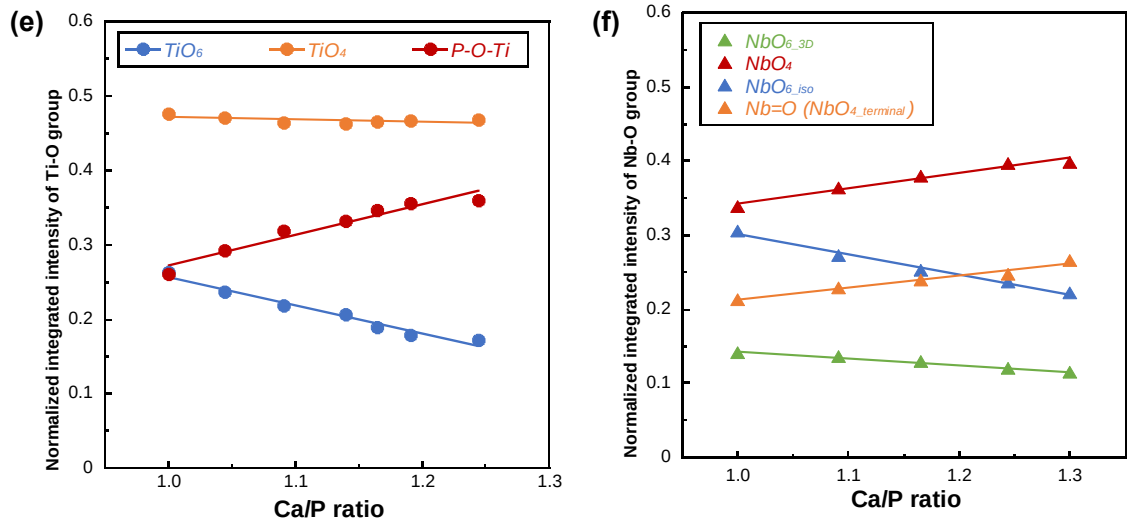
(e)
TiO6
TiO4
P-O-Ti
Normalized integrated intensity of Ti-O group
Ca/P ratio
(f)
NbO6_3D
NbO4
NbO6_iso
Nb=O (NbO4_terminal)
Normalized integrated intensity of Nb-O group
Ca/P ratio

3

4 Fig. 2

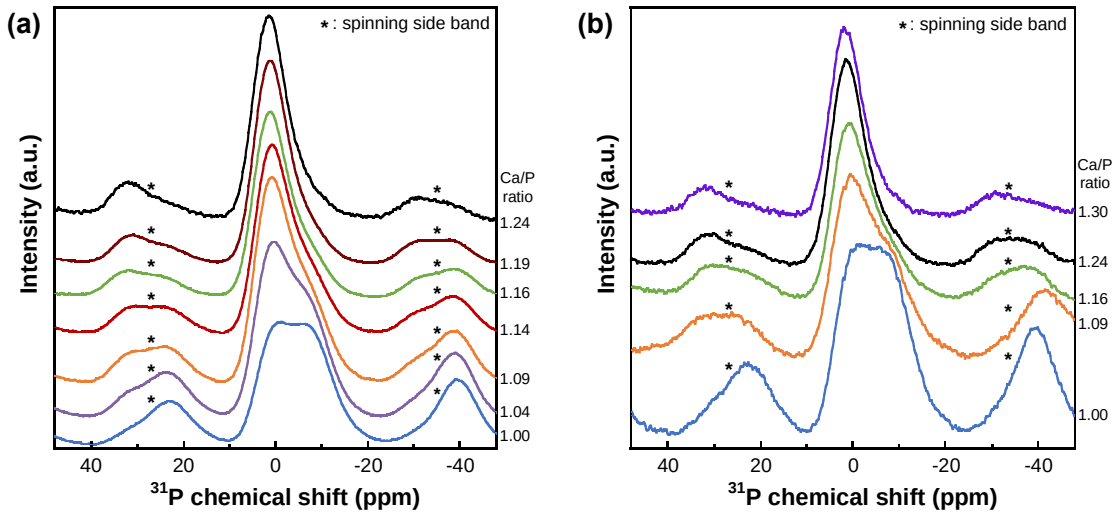
(a)
*: spinning side band
Intensity (a.u.)
Ca/P ratio
1.24
1.19
1.16
1.14
1.09
1.04
1.00
40
20
0
-20
-40
31P chemical shift (ppm)
(b)
*: spinning side band
Intensity (a.u.)
Ca/P ratio
1.30
1.24
1.16
1.09
1.00
40
20
0
-20
-40
31P chemical shift (ppm)

1

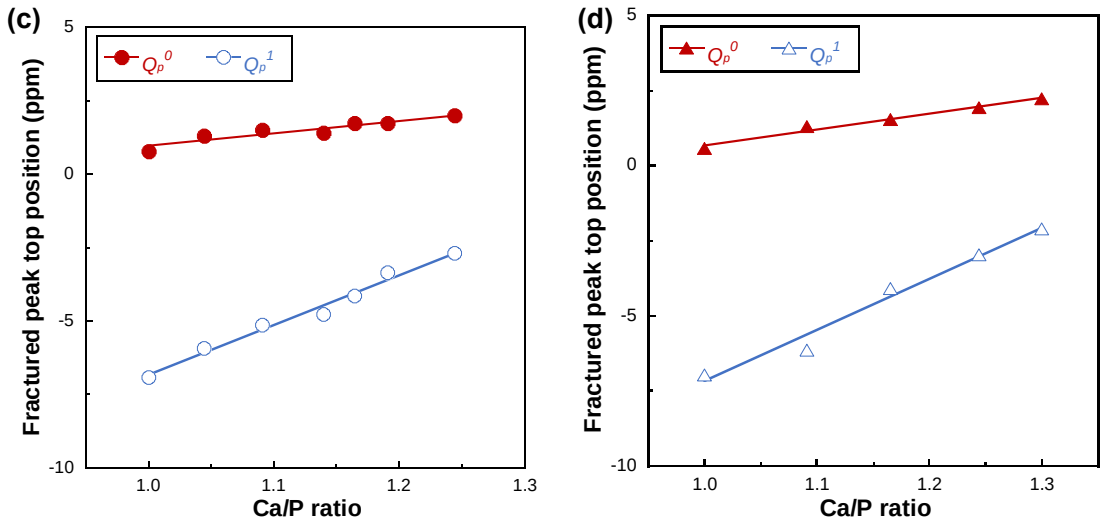
(c)
Qp0
Qp1
Fractured peak top position (ppm)
5
0
-5
-10
1.0
1.1
1.2
1.3
Ca/P ratio
(d)
Qp0
Qp1
Fractured peak top position (ppm)
5
0
-5
-10
1.0
1.1
1.2
1.3
Ca/P ratio

2

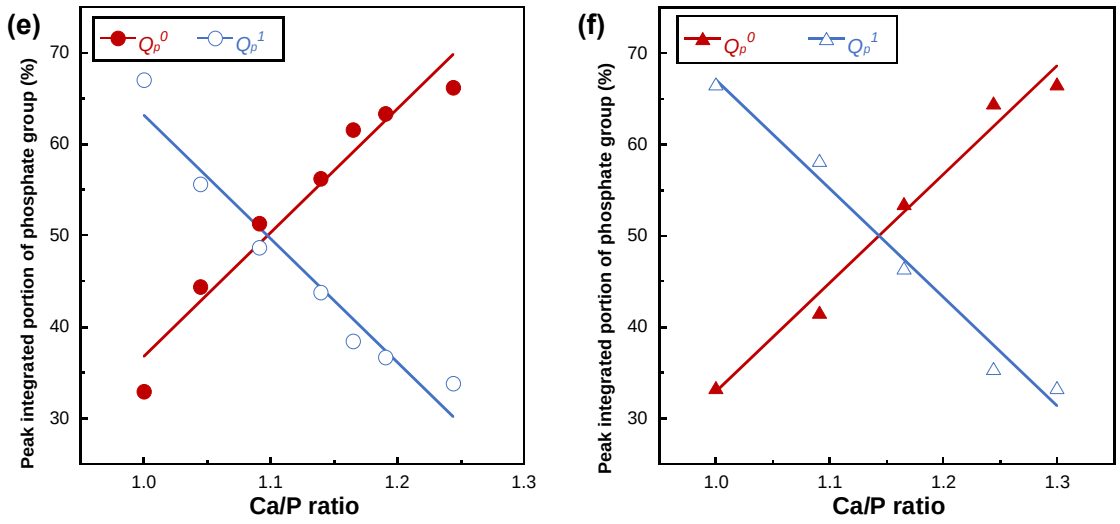
(e)
Qp0
Qp1
Peak integrated portion of phosphate group (%)
70
60
50
40
30
1.0
1.1
1.2
1.3
Ca/P ratio
(f)
Qp0
Qp1
Peak integrated portion of phosphate group (%)
70
60
50
40
30
1.0
1.1
1.2
1.3
Ca/P ratio

3

4 Fig. 3

1

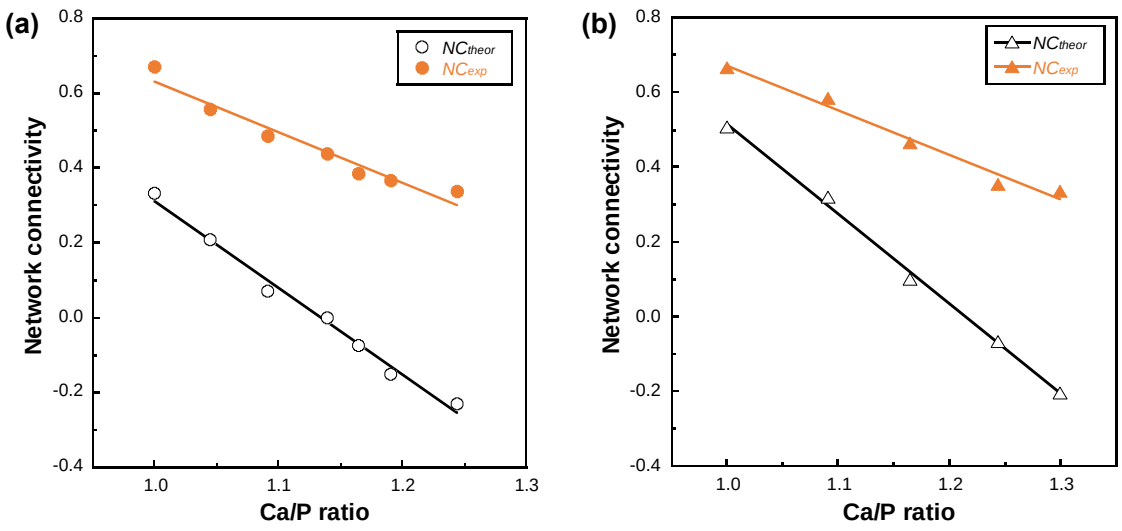
(a)
(b)
Network connectivity
Ca/P ratio
NCtheor
NCexp
0.8
0.6
0.4
0.2
0.0
-0.2
-0.4
1.0
1.1
1.2
1.3

2

3 Fig. 4

1

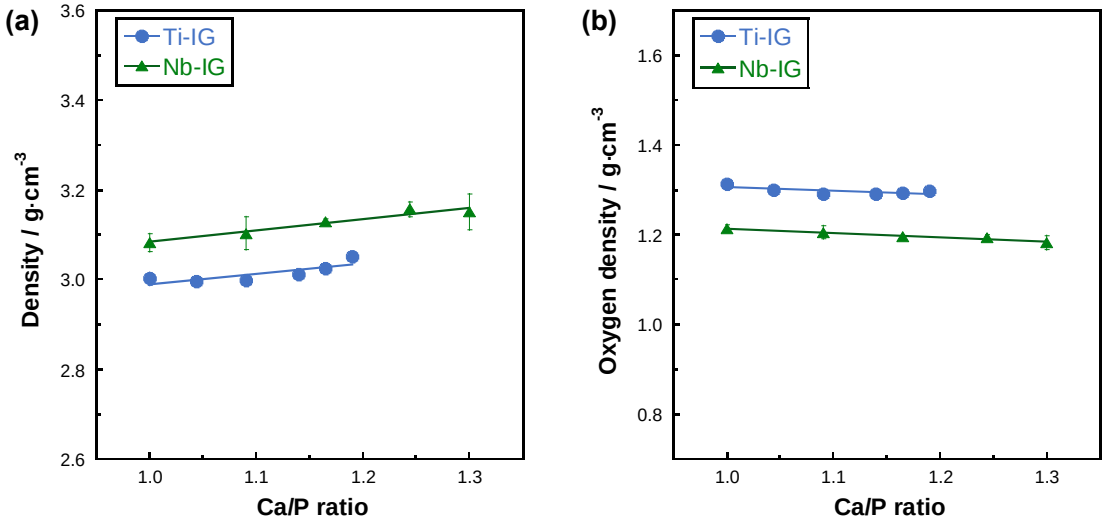
(a)
Ti-IG
Nb-IG
Density / g·cm-3
3.6
3.4
3.2
3.0
2.8
2.6
1.0
1.1
1.2
1.3
Ca/P ratio
(b)
Ti-IG
Nb-IG
Oxygen density / g·cm-3
1.6
1.4
1.2
1.0
0.8
1.0
1.1
1.2
1.3
Ca/P ratio

2

3 Fig. 5

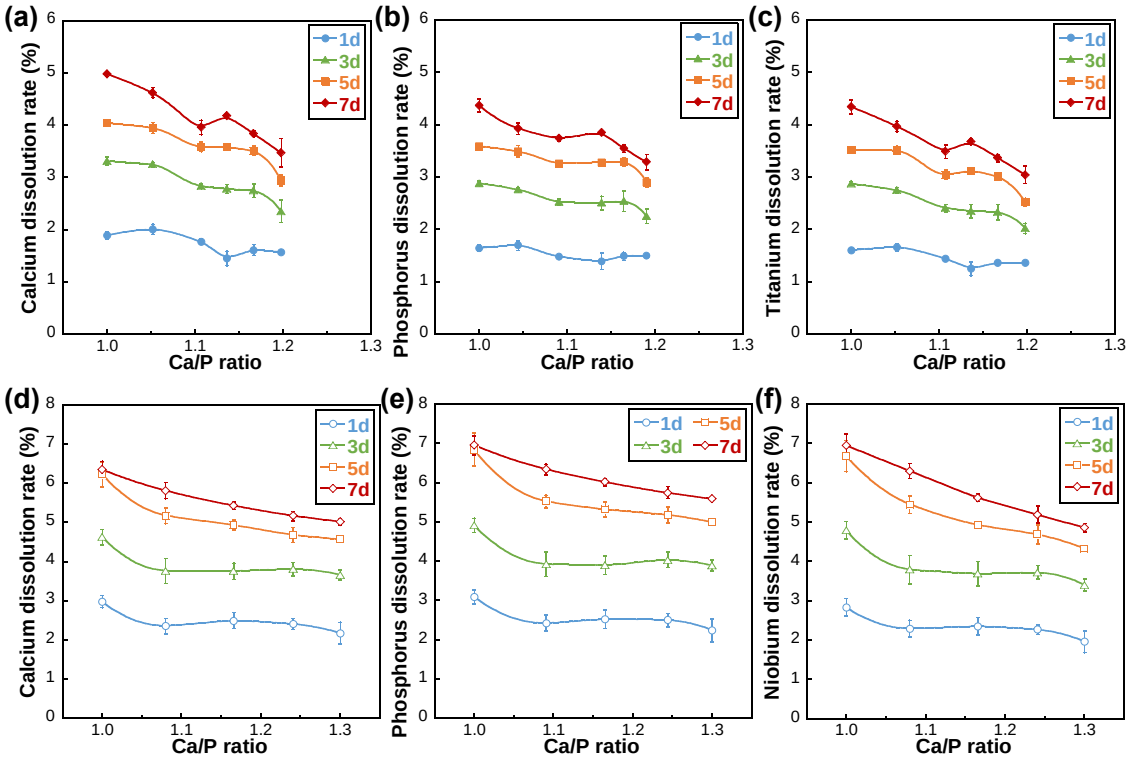
(a)
Calcium dissolution rate (%)
Ca/P ratio
(b)
Phosphorus dissolution rate (%)
Ca/P ratio
(c)
Titanium dissolution rate (%)
Ca/P ratio
(d)
Calcium dissolution rate (%)
Ca/P ratio
(e)
Phosphorus dissolution rate (%)
Ca/P ratio
(f)
Niobium dissolution rate (%)
Ca/P ratio
1d
3d
5d
7d

Fig. 6

Table

Table 1

Ca/P ratio (Glass code)		Composition / mol%				Composition / atom%			
		CaO	P_2O_5	TiO_2	Nb_2O_5	Ca	P	Ti	Nb
CaO-P_2O_5-TiO_2 Glasses (Ti-IGs)									
Partially crystalized ↑	1.00	60 (60.3±1.9)	30 (29.4±0.9)	10 (10.2±0.2)	-	46	46	8	-
	1.04	61 (61.6±1.3)	29 (27.9±0.4)	10 (10.5±0.2)	-	47	45	8	-
	1.09	62 (62.6±1.4)	28 (27.0±0.4)	10 (10.4±0.2)	-	48	44	8	-
	1.14	62.5 (63.1±1.3)	27.5 (26.4±0.5)	10 (10.5±0.2)	-	49	43	8	-
	1.16	63 (62.7±1.3)	27 (26.6±0.4)	10 (10.7±0.2)	-	49.5	42.5	8	-
	1.19	63.5 (63.7±1.2)	26.5 (25.7±0.4)	10 (10.6±0.2)	-	50	42	8	-
↓	1.24	64 (63.6±1.3)	26 (25.8±0.4)	10 (10.6±0.3)	-	51	41	8	-
CaO-P_2O_5-Nb_2O_5 Glasses (Nb-IGs)									
Partially Crystallized ↑	1.00	63 (62.1±1.5)	31.5 (30.5±0.8)	-	5.5 (7.3±0.6)	46	46	-	8
	1.09	65 (63.5±1.2)	29.5 (29.1±0.7)	-	5.5 (7.4±0.5)	48	44	-	8
	1.16	66.5 (63.4±0.5)	28 (28.6±0.4)	-	5.5 (8.0±0.1)	49.5	42.5	-	8
	1.24	67.5 (64.7±1.7)	27 (27.2±0.9)	-	5.5 (8.0±0.8)	51	41	-	8
↓	1.30	68.5 (64.8±0.3)	26 (26.9±0.1)	-	5.5 (8.2±0.1)	52	40	-	8

Analyzed compositions of Ti-IGs and Nb-IGs were obtained by ICP-AES and EDS, respectively.